SANDIA REPORT
SAND2022-12877
Printed September 2022

Sandia National Laboratories

Tracer Gas Model Development and Verification in PFLOTRAN

Matthew J. Paul, David E. Fukuyama, Rosemary C. Leone, Michael Nole, and Jeffery A. Greathouse

Prepared by
Sandia National Laboratories
Albuquerque, New Mexico
87185 and Livermore,
California 94550

Issued by Sandia National Laboratories, operated for the United States Department of Energy by National Technology & Engineering Solutions of Sandia, LLC.

Available to DOE and DOE contractors from
U.S. Department of Energy
Office of Scientific and Technical Information
P.O. Box 62
Oak Ridge, TN 37831

Telephone: (865) 576-8401
Facsimile: (865) 576-5728
E-Mail: reports@osti.gov
Online ordering: http://www.osti.gov/scitech

Available to the public from
U.S. Department of Commerce
National Technical Information Service
5301 Shawnee Rd
Alexandria, VA 22312

Telephone: (800) 553-6847
Facsimile: (703) 605-6900
E-Mail: orders@ntis.gov
Online order: https://classic.ntis.gov/help/order-methods/

ABSTRACT

Tracer gases, whether they are chemical or isotopic in nature, are useful tools in examining the flow and transport of gaseous or volatile species in the underground. One application is using detection of short-lived argon and xenon radionuclides to monitor for underground nuclear explosions. However, even chemically inert species, such as the noble gases, have bene observed to exhibit non-conservative behavior when flowing through porous media containing certain materials, such as zeolites, due to gas adsorption processes. This report details the model developed, implemented, and tested in the open source and massively parallel subsurface flow and transport simulator PFLOTRAN for future use in modeling the transport of adsorbing tracer gases.

ACKNOWLEDGEMENTS

The authors would like acknowledge Peter Lichtner and Glenn Hammond for insightful discussions on both the gas sorption and multi-continuum models implemented in PFLOTRAN. We additionally would like to recognize the work of all of the software developers that have contributed to the open-source PFLOTRAN project. Finally, we are grateful to Kris Kuhlman for providing a technical review of the work described herein.

This research was funded by the National Nuclear Security Administration, Defense Nuclear Nonproliferation Research and Development (NNSA DNN R&D). The authors acknowledge important interdisciplinary collaboration with scientists and engineers from LANL, LLNL, MSTS, PNNL, and SNL.

CONTENTS

LIST OF FIGURES

LIST OF TABLES

This page left blank

ACRONYMS AND TERMS

Acronym/Term	Definition
ADM	Advection-Dispersion Model
BET	Brunauer-Emmett-Teller
DCDM	Dual Continuum Disconnected Matrix
FWHM	Full Width at Half Maximum
IUPAC	International Union of Pure and Applied Chemistry
NPE	Non-Proliferation Experiment
NGME	Noble Gas Migration Experiment
PFAS	Per- and Polyfluoroalkyl Substances
PFLOTRAN	Parallel Flow and Transport
UNE	Underground Nuclear Explosion
VOC	Volatile Organic Compound

This page left blank

1. INTRODUCTION

Isotopes of noble gases [1] and inert chemical tracer gases are used to characterize the air flow in the surface [2], as well in the subsurface, to characterize mine ventilation [3] and air flow for nuclear waste disposal [4]. More pertinent to this work, they have also been utilized to simulate the transport of fission and activation products produced by underground nuclear explosions (UNE), such as the Non-Proliferation Experiment (NPE) [5] [6] and the Noble Gas Migration Experiment (NGME) [7] [8]. A common assumption is that these tracer gases are conservative, and by that, their total mass in the gas phase is a constant. However, no gas is truly an ideal or perfect gas, with each chemical species having varying degrees of intermolecular interactions with other gases, liquids, and solids.

Sorption is the generic term given to the phenomenon of both absorption – that is solvation into a bulk liquid or solid – and adsorption, which results in condensation of the gas onto solid surfaces. Gas absorption – also known as solubility – has been systematically studied and documented by the International Union of Pure and Applied Chemistry (IUPAC) and the National Institute of Standards and Technology for the many tracer gases of interest in water and other common solvents [9]. Similarly, gas absorption or solubility is widely supported in existing subsurface flow and transport simulations, including PFLOTRAN [10], and is referred to here to compare to the gas adsorption model developed herein.

Gas adsorption is the process by which gas molecules condense onto a solid surface. This occurs because the chemical potential of gases near a surface differs from the bulk regions due the intermolecular forces of the solid phase [11]. This results in observable fluid densities in excess of the free gas density [12]. Depending on the strength of the intermolecular forces, the process is categorized as chemical or physical adsorption, which influences the appropriate adsorption model. For gases below their critical temperature, this process can be a precursor to capillary condensation. However, adsorption is nevertheless distinct from liquid condensation as gases above their critical temperature can form a condensed adsorbed phase [13]. In this way, seemingly inert and presumed conservative tracer gases, including Xe [14] and SF_6 [15] can appreciably adsorb onto naturally occurring geological materials at ambient subsurface temperatures. However, the relative quantity that is adsorbed versus free in a porous matrix is highly dependent both on the mineralogy and the specific surface area of the porous medium.

To that effect, gas adsorption is only significant in some geological materials. Prior to developing this capability, intact heterogeneous rock samples were analyzed with a novel piezometric method [16], indicating the significant differences in gas properties between samples taken at Blue Canyon Dome and Aqueduct Mesa, both sites of field tests using tracer gases. While effectively 100% of Ar and Xe in the Blue Canyon Dome sample remained in the gas phase, only 25% of the Ar and 5% of the Xe remained in the gas phase in the zeolitized tuff from Aqueduct Mesa. While this difference is large, this is indicative of the zeolite minerals content, and highlights the need to have gas adsorption capabilities to model particular geologies [17].

Whereas these previous tests using noble gases were conducted using a single-component gas phase, recent results from Los Alamos National Laboratory suggest non-conservative behavior persist in partially water saturated, air-water systems [18]. However, quantifying this adsorption in multicomponent environments is technically challenging as conventional instruments are only capable of single-component measurements. Note that water vapor is then one of the components if the sample is partially water saturated. Experimental efforts are being conducted in parallel to this model development with results that are documented in an upcoming report.

Section 2 details the gas adsorption model developed for the subsurface flow and transport simulator, PFLOTRAN, discussing its assumptions and limitations. Section 3 details verification of this model against a simple but analytical model. In addition to the gas adsorption work highlighted here, additional model development work was conducted to develop gas transport within the multi-continuum model in PFLOTRAN. This has the potential to reduce the computational complexity relative to discrete fracture networks and a demonstration of this capability for modeling barometric pumping is discussed in Section 4.

2. TRACER GAS MODEL

To implement a tracer gas adsorption model in PFLOTRAN requires a background on the prior model. PFLOTRAN and many similar subsurface simulators, sequentially solve the "flow" of the solvent or carrier phases, followed by the "transport" of the solute or tracer species. In reality, both "flow" and "transport" are mass balances, but with different expressions for the mass flux.

In the vadose or unsaturated zone, two phases are generally present, the liquid, which is predominantly water, and the gas, which is predominantly air. While some air is solvated into the liquid phase, and some water vapor is present in the gas phase, under the local equilibrium assumption, the concentration of each in the complementary phase is fixed by solubility and vapor pressure tables when both liquid and gas phases are present. Thus, water and air in the liquid and the gas phases can be approximately modeled using only two "flow" mass balances.

Transport species differ from flow species as they negligibly contribute to the overall mass and mechanical balance of the system. While they are advected by and diffuse through the prevailing flow (solvent) species, they must not be present in concentrations sufficient to appreciable alter flow. Thus, the fundamental requirement of a sequential flow and transport solver is that all "transport" species are dilute relative to the "flow" species.

For many dissolved solutes in the aqueous phase, this requirement is universally satisfied as their concentration is limited by solubility in the aqueous phase. However, a defining characteristic of the gaseous phase is that all gas species are fully miscible with all other gases. Consequently, there is no constant delineation between "flow" and "transport" species in the gas phase. As this work focuses on the very low concentrations expected for isotopic chemical tracers, the scarcity of the tracer gas relative to ambient air is sufficient to allow for the dilute transport approximation.

2.1. Gaseous Flow

The air component of the gas phase in PFLOTRAN air is a mixture of many species, mostly nitrogen, oxygen, and argon. In most simulations, separating air mixtures according to their different solubilities or diffusivities is not of interest and the conglomerated pseudo-species air is assumed to exist only in a fixed proportion. This prevents the need for separate mass balances for nitrogen, oxygen, argon, and other minor components of air. Thus, gases like He, Ne, Kr, and Xe that are present in air, albeit at low concentrations, are implicitly modeled by the pseudo-species air.

In doing so, the velocity of the gas phase q_g is then calculated using a generalized version of Darcy's law for two-phase flow. The dynamic viscosity of the air-water vapor mixture is μ, while the intrinsic and relative permeability are κ and k_{rg}, respectively. The superficial flow velocity is then proportional to the pressure gradient ∇P.

$$q_g = \frac{\kappa k_{rg}}{\mu} \nabla P$$

Because flow and transport are solved sequentially, the subsequent advection-diffusion transport solution is found using a fixed velocity from the flow solution for each transport time step.

2.2. Gaseous Transport

There are broadly, two types of tracer gases of interest here. The first type is isotopic tracers, which are naturally occurring chemical species in air. Isotopic tracers have nearly identical chemical and physical properties and are primarily distinguished by their nuclear properties, such as mass. The second type is chemical tracers. These tracers are chemicals that are not naturally occurring at any appreciable abundance. These have very low natural background levels but have different physical chemical properties than naturally occurring gases. There are advantages and disadvantages for each type of tracer depending upon the application.

Isotopic tracers can be further divided into stable and radioactive versions. Stable isotopes can be utilized if they are found only at low background concentrations. For example, in the NPE, ^{3}He was released [5] [6]. And while high levels of ^{4}He are naturally occurring, ^{3}He is found only at trace background levels. Thus, the arrival of a plume of ^{3}He can be observed using mass spectrometry.

Radionuclide tracers are isotopic tracers with the added benefit of typically having vanishingly low background levels and high sensitivities using radiation counting methods. Two such tracers include ^{37}Ar and ^{127}Xe, which were utilized by the NGME [7] [8]. While significant amounts of predominately ^{40}Ar will coexist with the ^{37}Ar, only the ^{37}Ar should be modeled in transport as the naturally occurring isotopes – ^{36}Ar, ^{38}Ar, and ^{40}Ar – are implicitly modeled in flow.

Chemical tracers, such as SF_6, which was utilized in both the NPE and NGME tests, do not exist in the natural background at any appreciable level. The primary advantage of chemical tracers is that they can be used by chemically sensitive techniques, such as gas chromatography. While this necessitates larger quantities of these tracers to be injected relative to isotopic tracers, SF_6 is particularly useful as it has detection thresholds as low as parts per trillion [19]. The primary disadvantage of chemical tracers is that they do not accurately represent the chemical properties of the radionuclide species of interest for underground nuclear monitoring. That is, the arrival time of ^{37}Ar and ^{133}Xe may not be accurately interpolated from ^{3}He and SF_6 arrival scaling by diffusivity alone.

In PFLOTRAN, the transport flux Ω_j^α of the species j in phase α is defined using the Advection-Diffusion Model (ADM). In the ADM, the advective flux is calculated as the product of solute concentration in the gas phase Ψ_j^g, and the flow gas phase velocity q_g. The diffusive flux acts in parallel and is modeled as the product of the concentration gradient, porosity φ, gas phase saturation s_g, and a Fickian diffusion coefficient D_g.

$$\Omega_j^\alpha = \left(q_g - \varphi s_g D_g \nabla\right)\Psi_j^\alpha$$

Additionally, it is cautioned that while the ADM is satisfactory for the transport of tracer species in continuum flow, deviation from this behavior occurs in rarefied flow. Rarefied flow occurs when the mean free path of the transport species is comparable to the pore dimensions. This occurs at atmospheric pressure in media with pores on the order of 1 μm or less, which is prevalent in multiple lithologies at the Nevada National Security Site [20]. These scenarios can require more comprehensive models, such as the Dusty Gas Model [21], but few subsurface flow and transport simulators presently have this capability.

The transport flux described above can then be algebraically substituted into the transport mass balances. This results in the implemented transport mass balance [10]

$$\frac{\partial}{\partial t}\left(\varphi \sum_{\alpha} s_{\alpha}\Psi_j^{\alpha}\right) + \nabla \cdot \sum_{\alpha} \Omega_j^{\alpha} = Q_j - \sum_{\alpha} v_{jm} I_m - \frac{\partial S_j}{\partial t}.$$

Here, the time derivative $\frac{\partial}{\partial t}$ represents transient accumulation and depletion of a species, indexed by j and given as the sum of the volumetric concentrations ψ_j^{α} in all phases indexed by α. The fractional volume of the phase is given by the degree of saturation s_{α}, which is, itself the fraction of the porosity, φ, occupied by a given phase. The region of a representative elementary volume occupied by the solid phase is complementary to porosity and is assumed devoid of the species j.

On the opposite side of the mass balance are the so-called reactive terms. Q_j and $\sum_{\alpha} v_{jm} I_m$ have been used to model various reactions, including radioactive decay or mineral precipitation and dissolution. While Q_j plays an important role in radionuclide transport, modeling radioactive decay is not necessary for validating the gas adsorption model and will be omitted from further discussion.

The final term $\frac{\partial S_j}{\partial t}$ has previously been used to represent adsorption and desorption processes in the liquid phase. If the rates of adsorption and desorption are kinetically limited, a separate adsorbed phase mass balance may be necessary. However, if the adsorbed phase is assumed to be in a local equilibrium, or approximately so, the mass balance can be rearranged such that the adsorbed phase appears within the transient accumulation term and is only marginally different than a bulk liquid or gas phase in equilibrium. The validity of the local equilibrium model depends upon the time and volume discretization, in addition to material properties.

In the vadose zone, there are typically only two bulk fluid phases, the liquid (l) phase and the gas (g) phase. Compared with the gas phase velocity, the liquid phase is assumed to be scarcely perturbed by fluctuations in barometric pressures. Consequently, this report does not detail transport of sorbed gas in the aqueous phase, as the liquid phase is assumed to be relatively stagnant compared to air. Nevertheless, the stagnant liquid phase retained as capillary water is nevertheless important as is occupies pore volume and affects the water vapor pressure. PFLOTRAN assumes the gas phase saturation is the complement to the liquid phase saturation. I.e., $S_g = 1 - S_l$.

Following this framework, this work has introduced the additional adsorbed phase due to adsorption directly out of the gas phase. Herein, it will be denoted with a superscript s to represent it as the material adsorbed to the solid surface. The volume of the solid phase is complementary to the porosity, that is $(1 - \varphi)$. As a surface phase, equilibrium is reached when the areal concentration of the adsorbed phase is in equilibrium with the volumetric concentration of the fluid phase. However, the specific surface area of most materials is rarely known, and a customary assumption is that the surface area is proportional to the mass. Consequently, the adsorbed concentration Ψ_j^s will be expressed on a gravimetric basis. The adsorbed quantity can then be expressed as the product of solid volume, skeletal density ρ^S, and gravimetric concentration. Replacing the summation with explicit liquid, gas, and solid phases enables the transport mass balance for stable tracer gases to be expressed more directly, as below.

$$\frac{\partial}{\partial t}\Big((1-\varphi)\rho^s\Psi_j^s + \varphi\Big(S_l\Psi_j^l + (1-S_l)\Psi_j^g\Big)\Big) + \nabla \cdot \Omega_j^g = 0$$

2.3. Gas Sorption

Thus far, the concentration of the liquid, gas, and adsorbed phases has been presented as three separate quantities. However, under the local equilibrium assumption, the number of degrees of freedom is reduced by each additional phases present, as per the Gibbs phase rule. Thus, while there is an additional adsorbed phase concentration in each control volume, under the local equilibrium assumption, no additional degrees of freedom are introduced.

Here, the tracer gases are assumed to be adequately modeled by the ideal gas equation of state. As such, the partial pressure of the gas is directly proportional to the gas phase Gibbs free energy. Where appropriate, equilibrium between the gas, liquid, and adsorbed phase equilibria can be effectively modeled with minimal complexity.

2.3.1. Gas-Liquid Equilibria

For a multicomponent system, the composition of the gas and liquid phases are dissimilar, with the more volatile component being present in a greater proportion in the gas phase. For an ideal solution, intermolecular forces between the different transport components are negligible and the partial pressure of a species in the gas phase is proportional to its mole fraction x_j in solution and the pure component vapor pressure P_j^{vap}. This is known as Raoult's Law.

$$p_j = x_j P_j^{\mathrm{vap}}$$

However, many liquid solutions have some degree of intermolecular interaction that can either stabilize or destabilize a solution. The degree of non-ideality is represented using an additional activity coefficient γ_j that relates the increase or decrease the partial pressure in the gas phase relative to an ideal solution.

$$p_j = x_j \gamma_j P_j^{\mathrm{vap}}$$

In practice, the activity coefficient can have complex relationships in multicomponent solutions. Nevertheless, in the dilute limit, the activity coefficient always approaches a finite value for a given solvent. Also in the dilute limit, the mole fraction of a solute j negligibly affects the density of the overall solution such that the mole fraction can be related to the mass concentration in the liquid. This enables the partial pressure for a dilute solution to be modeled using a Henry's Law coefficient $\mathcal{H}_j^l$.

$$\lim_{x_j \to 0} x_j \gamma_j P_j^{\mathrm{vap}} \to \mathcal{H}_j^l \Psi_j^l = p_j$$

Henry's Law also applies to the solvation of permanent gases. Permanent gases here are those species that are above their critical temperature such that there is no stable liquid phase at any pressure. Despite having a theoretically infinite vapor pressure, permanent gases can appreciably absorb into aqueous solutions because the solution is non-ideal. This is observed with nitrogen and oxygen in air, which are similarly modeled via Henry's Law.

PFLOTRAN transport makes no distinction between vapors and permanent gases in the transport model as Henry's Law is an appropriate for all dilute solutions. For example, the tracer gas SF_6 is technically a vapor below the critical temperature of 45.5 °C. Xe is very near its critical temperature of 16.6 °C in subsurface models. In any case, Raoult's Law would overestimate the solubility of SF_6 in liquid water, as the non-polar SF_6 is unstable in a polar solvent like water. At the same time, Raoult's Law would underestimate the solubility of Xe in an aqueous solution, as Xe is not by itself

polar, but is polarizable and soluble in water. Assuming the ideal gas equation of state, the partial pressure of a gas species can be readily related to the gas phase concentration. Thus, expressing Henry's Law in terms of volumetric concentration:

$$\Psi_j^g = \frac{p_i}{RT} = \frac{\mathcal{H}_i^\ell}{RT}\Psi_i^\ell$$

2.3.2. Gas-Solid Equilibria

The underlying thermodynamics of adsorption are comparable to that of liquid-vapor and gas absorption equilibria. Again, the Gibbs free energy of the gas is proportional to the partial pressure. However, the Gibbs free energy of a gas molecule near a solid surface is lower near the surface of a solid due to the chemical environment imposed by the solid surface. Due to pore sizes, there can be additional steric or size selection effects, which greatly alter the adsorption of specific chemical species. The primary difference is that the adsorbed gas is restricted to the surface and thus it is the surface concentration and not volumetric concentration that is related to the partial pressure.

The gas concentration in liquids is typically low enough such that solvated species do not interact with each other. However, as the adsorbed phase is limited in extent, competition for the limited surface sites is more prevalent. In single-component measurement, the only competition is with other molecules of the same gas species. To measure this effect, gas adsorption measurements are typically made with a single gas over a range of pressures at a given temperature to evaluate the adsorption function f at a given temperature T, and is called an isotherm. Here, we generically will express the adsorption function as a function of both temperature and species pressure p_j:

$$\Psi_j^s = f(T,p_j)$$

At low surface coverages, the adsorption isotherm is linear with gas pressure and follows Henry's Law [22]. If the gas only adsorbs as a monolayer, the Langmuir adsorption model, with a limited number of absorption sites, is appropriate [11]. For gases below their critical temperature, capillary condensation can occur, and the BET model is more appropriate [13]. At low surface coverage, the Langmuir and BET isotherms can both adequately fit data, and it is only when extrapolating to higher surface coverages that divergence between the monolayer and multilayer adsorption models is apparent. Seiman *et al.* illustrated this behavior when modeling the adsorption of nerve agent degradation products to soil [23].

Furthermore, as the solid phase is itself heterogeneous, the empirically formulated Freundlich isotherm is often appropriate [24]. In practice, the Henry's Law model has the greatest applicability to tracer gas transport due to the dilute requirement, as was discussed by Barrer [22]. Its application to multicomponent systems will be detailed here.

2.3.3. Multicomponent Linearization

As mentioned, Henry, Langmuir, Freundlich, and BET models are all developed for single component environments and do not, by themselves, account for competition for adsorption sites with other gas species that may be present. Thus, a more complete representation of the adsorbed phase concentration in a multicomponent system would require an adsorption function model that accounts for the partial pressure p of each of the N gas components:

$$\Psi_i^s = f(T,p_i, \ldots,p_N)$$

Systems with widely varying composition may require a more comprehensive solution, such as Ideal Adsorbed Solution Theory [25]. However, even this can be erroneous for microporous adsorbents, such as zeolites [26].

Instead, as this work is limited to dilute transport, two approximations to the multivariate adsorption function can be made. First, it has already been required that interactions amongst the tracer gases must be negligible. The adsorption function need only be parameterized for the particular transport species and the flow species present. And second, because of the pseudo-species air is found only in constant proportions, the adsorption function necessary to model tracer gas transport is a function of air, water vapor, and tracer pressures only.

$$\Psi_i^s \cong f(T, p_i, p_{air}, p_{H_2O})$$

Furthermore, while the air pressure, water vapor pressure, and temperature are not strictly constant during barometric pumping scenarios, these undergo only small fluctuations around the average values. Thus, to estimate the adsorbed concentration of the tracer gas i in such an environment, a Taylor series expansion can be performed along tracer partial pressure alone.

In the simplest case, a chemical tracer is utilized which has negligible background concentration in the flow carrier gas. In this scenario,

$$\Psi_i^s \cong 0 + \frac{df(T, 0, p_{O_2}, p_{Ar}, p_{H_2O})}{dp_t} p_t + \dots$$

This is simply a restatement of Henry's Law as if the surface has modified surface chemistry:

$$\Psi_t^s = \frac{df(T, p_{N_2}, p_{O_2}, p_{Ar}, p_{H_2O})}{dp_t} p_t$$

For an isotopic tracer, such as ^{37}Ar, there is, however, a large partial pressure of naturally occurring Ar, in addition to the tracer gas. Thus, for this approximation, let p_t be the tracer gas partial pressure and p_b be the background pressure in air. The net concentration of the chemical species adsorbed is thus the summation of the tracer and background components Ψ_{t+b}^s.

$$\Psi_{t+b}^s = f_{Ar}(T, p_{N_2}, p_{O_2}, p_{Ar} + p_t, p_{H_2O})$$

Performing a Taylor expansion around the background pressure for a perturbation, the magnitude of the tracer pressure is

$$\Psi_{t+b}^s = f(T, p_{N_2}, p_{O_2}, p_{Ar}, p_{H_2O}) + \frac{df(T, p_{N_2}, p_{O_2}, p_{Ar}, p_{H_2O})}{dp_{Ar}} p_t + \dots$$

While the total concentration of the sorbed chemical species is the summation of the background and the isotopic tracer, the sorbed tracer is not simply the marginal amount sorbed. Rather, because the gas and sorbed phases are in dynamic equilibrium, the isotopic tracer is mixed in with the naturally occurring species. Local equilibrium is reached when the isotopic abundance in the gas phase is equal to the isotopic abundance in the sorbed phase. Slight isotopic shifts in vapor pressure due to differences in molecular weight can occur but are not being modeled here. Thus, the adsorbed concentration of only the isotopic tracer can be calculated as product of the total sorbed concentration and the isotopic abundance in the gas phase.

$$\Psi_t^s = \Psi_{t+b}^s \frac{p_t}{p_t + p_b}$$

Substituting in the Taylor series expression for the sorbed concentration results in

$$\Psi_t^s = f(T,p_{N_2},p_{O_2},p_{Ar},p_{H_2O})\frac{p_t}{p_t+p_b} + \frac{df(T,p_{N_2},p_{O_2},p_{Ar},p_{H_2O})}{dp_{Ar}}\frac{p_t^2}{p_t+p_b} + \ldots$$

Thus, due to dynamic equilibrium, the magnitude of the adsorption function under the prevailing flow composition is of primary importance while the derivative or marginal quantity sorbed is secondary.

$$\Psi_t^s = \frac{f(T,p_{N_2},p_{O_2},p_{Ar},p_{H_2O})}{p_b}p_t + \ldots$$

Consequently, whether chemical or isotopic tracers are utilized, the adsorption function can be effectively linear over the narrow range of concentrations relevant to tracer gas transport.

2.4. Retention Factor Approach

While the adsorption function relates the concentrations of adsorbed phases, the finite volume method requires that quantities, not concentrations, be related. As such, the adsorbed phase concentration is always multiplied by the solid fractional volume and skeletal density. Thus, the fractional volume of the solid, the grain density, and the linear isotherm can be combined into a single dimensionless quantity. Using IUPAC nomenclature, this quantity is the "retention factor", expressed here as r_j, which describes the relative quantities in the stationary and mobile phases. In this case, these phases are adsorbed and gaseous.

$$r_j = \frac{\text{adsorbed quantity}}{\text{gaseous quantity}} = \frac{(1-\varphi)\rho^s\Psi_j^s}{\varphi\Psi_j^g} = \frac{(1-\varphi)\rho k_j^s RT}{\varphi}$$

This is related to the "retardation" factor R_j used in the geosciences, which is defined as the total quantity over the mobile quantity. However, the IUPAC definition of the retardation factor is the multiplicative inverse of the geoscience retardation factor. Because of the ambiguity in the definition of the retardation factor, the retention factor has been selected as the preferred nomenclature here.

$$R_j = \frac{\text{adsorbed quantity} + \text{gaseous quantity}}{\text{gaseous quantity}} = 1 + r_j$$

Using the retention factor approach, the finite volume approach can be rewritten to correlate the gas and adsorbed phase quantities.

$$\frac{\partial}{\partial t}\Big(\varphi\Big(s_l\Psi_j^l + (1-s_l)\big(1+r_j\big)\psi_j^g\Big)\Big)\Delta V + \sum_\alpha \Omega_j^\alpha \cdot \Delta A = 0$$

Thus, the retention factor appears as a perturbation to the apparent volume of the gas phase saturation. This fits well within the existing PFLOTRAN implementation and allows for an efficient implementation of the gas adsorption model.

In many cases, the porosity, skeletal density, and adsorption coefficient for a given rock matrix are not independently known, yet the combined effect can be observed from advection or sorption experiments. The retention factor allows a modeler to hold the proportion of gas observed constant while conducting simulations over a range of porosities and vice versa. This feature can be advantageous to conduct parametric studies on gas arrival times with uncertain matrix properties.

This page left blank

3. MODEL VERIFICATION

To verify the implementation satisfies the presented model, results of PFLOTRAN simulations are being compared to a known analytical solution. In this test scenario, unidirectional and uniform flow is specified in the flow model. The liquid phase saturation is set to near residual such that there is no appreciable liquid flow. Additionally, a tracer plume is inserted in a single cell of a one-dimensional model at the initial time zero.

In this scenario, the mass balance for the transport model can be expressed with the one-dimensional advective-diffusive equation.

$$\frac{\partial(1+r)\psi}{\partial t} - \frac{\partial u\psi}{\partial x} + \frac{\partial}{\partial x}\left(D\frac{\partial \psi}{\partial x}\right) = 0$$

If the retention factor, velocity, and diffusivity are uniform, these coefficients are excluded from the derivatives. This enables the equation to be expressed as a second order but linear and homogenous partial differential equation.

$$(1+r)\frac{\partial \psi}{\partial t} - u\frac{\partial \psi}{\partial x} + D\frac{\partial^2 \psi}{\partial x^2} = 0$$

The solution to this equation for a point source (i.e., its Green's function) is the well-known Gaussian distribution.

$$\psi(\xi,t) = \frac{\psi_0}{\sigma\sqrt{2\pi}} e^{-\frac{\xi^2}{2\sigma^2}}$$

Where the tracer peak location is determined by $\xi = x - \frac{u}{1+r}t$ and the tracer peak width grows to a standard deviation $\sigma = \sqrt{\frac{2Dt}{1+r}}$. While this is a simple analytical solution, it enables two essential performance metrics to be readily confirmed.

1. Retarded Advection. For a non-sorbing tracer, the tracer maximum travel with the same superficial velocity as the carrier gas flow model. However, for non-zero retention factors, the location of the maximum peak must travel with a velocity of $\frac{u}{1+r}$.
2. Contracted Diffusion. The point source must approach a Gaussian distribution with increasing time. The full width at half maximum (FWHM) will increase with the square root of time and diffusivity, but it will be reduced by a factor of $1+r$.

Both performance metrics will be verified herein using the unidirectional and homogeneous model. In the following subsections, results obtained from simulations conducted using Xe as a tracer gas beginning at 10 m from the left edge of a 110 m domain. The bulk gas phase velocity is approximately $2.7 \cdot 10^{-5}$ m/s and the SF_6 diffusivity in air is fixed at 0.124 cm^2/s. The retention factors utilized here form a parametric set and do not correspond to any particular lithologies.

3.1. Retarded Advection

From the Green's function solution, it is predicted that the velocity of an adsorbing tracer peak will be retarded relative to the air carrier gas by a factor of $1+r$. By calculating the displacement of the peak maximum from the source location, the velocity of the tracer peak can be readily found. The tracer gas concentration profile with time, as well as the location of the peak, are plotted in Figure 3-1. Table 3-1 lists the fitted velocity over a range of retention factors modeled, as well as the

normalized velocity to the un-retarded peak. As indicated, the normalized velocities are in excellent agreement with the analytical solution.

Table 3-1. Tracer Peak Velocity

Retention Factor	Velocity (m/s)	Relative Velocity	$\frac{1}{1+r}$
0	2.44×10^{-5}	1	1
0.1	2.218×10^{-5}	0.909	0.9091
0.5	1.627×10^{-5}	0.667	0.6667
1.0	1.22×10^{-5}	0.500	0.5000
10	2.22×10^{-6}	0.0909	0.0909

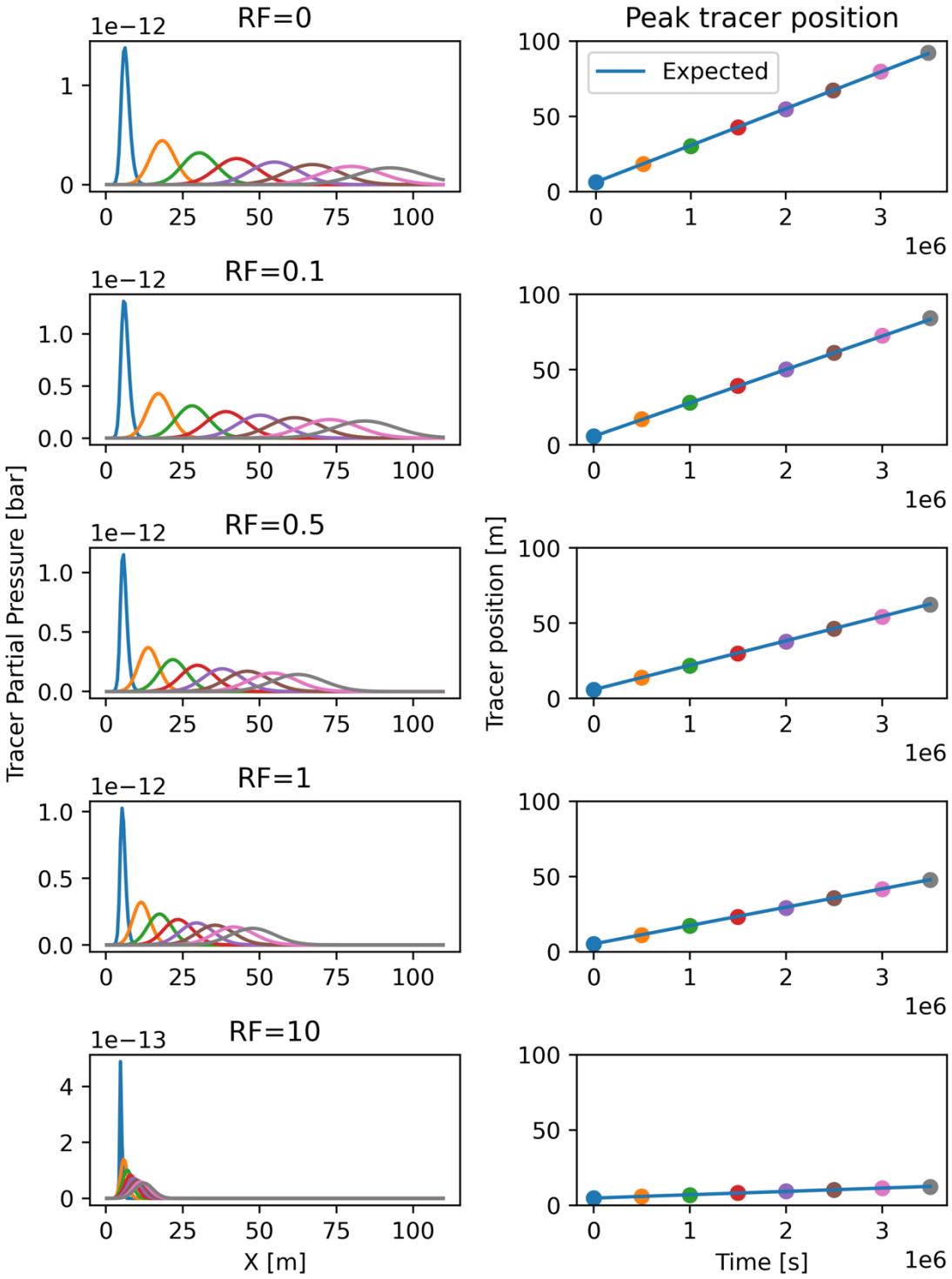

Figure 3-1. Tracer Peak Position versus Time and Retention Factor

3.2. Contracted Diffusion

Lastly, the width of the tracer peak with time is compared to verify the effects of the retention factor on diffusivity. The FWHM is utilized here to quantify peak width. The FWHM of a gaussian peak is a constant multiple of the standard deviation.

$$FWHM = 2\sqrt{2\ln(2)}\,\sigma = 4\sqrt{\frac{\ln(2)\,Dt}{1+r}}$$

Because PFLOTRAN uses a finite volume approach, the tracer peak must begin with an initial peak with the size of the control volume and cannot perfectly represent a Dirac delta function. Nevertheless, with increasing simulation time, the peak broadens, spanning more elements and approaches an idealized Gaussian peak shape. Thus, while there is some slight variation in peak width early in each simulation, they all broaden in accordance with the square root of time. Figure 3-2 illustrates this by plotting the squared FWHM, resulting in nearly linear correlations with time.

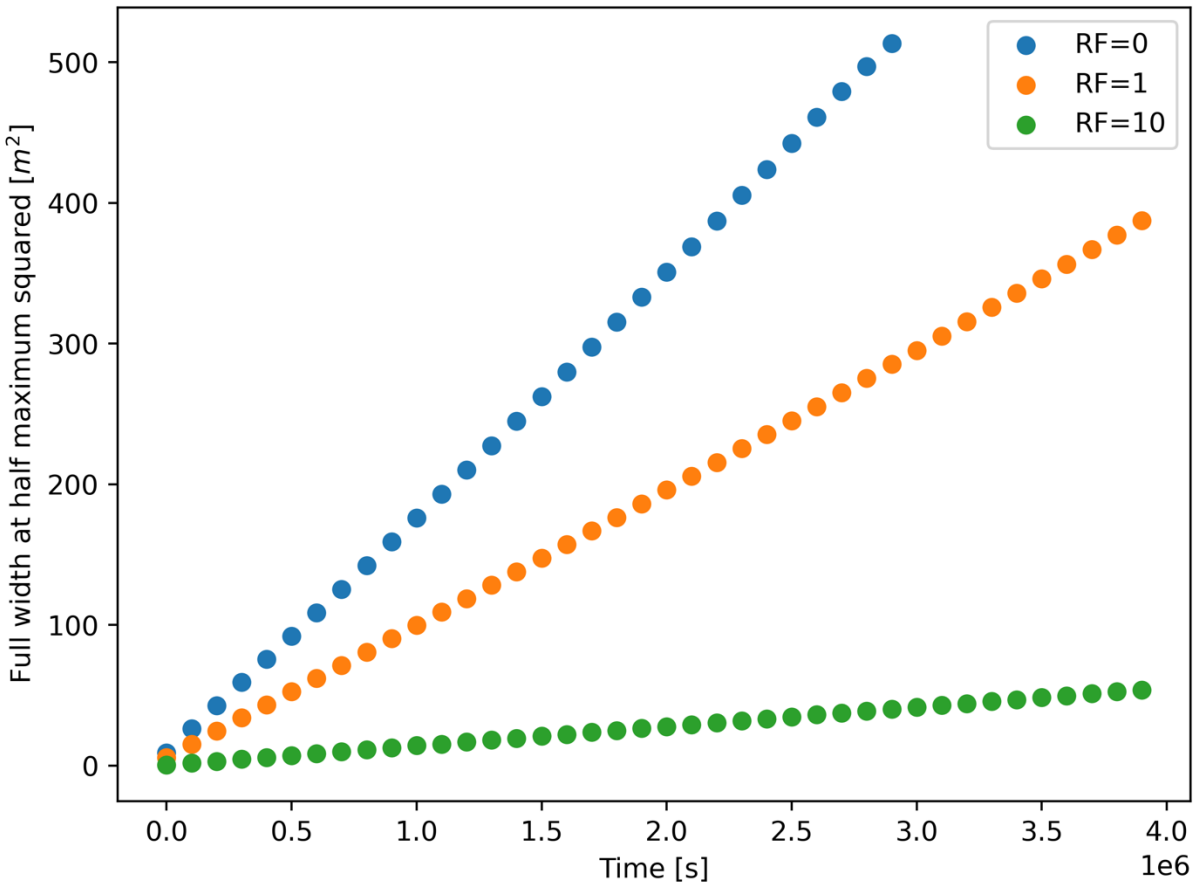

Figure 3-2. Tracer Peak Width Squared versus Time and Retention Factor

4. MULTICONTINUUM MODEL DEVELOPMENT

The multiple continuum model in PFLOTRAN allows for representation of fracture-matrix interactions in a dual porosity system, making it ideal to model barometric pumping-which occurs in a domain with highly permeable fractures surrounded by a low permeability matrix. PFLOTRAN simulates a dual porosity system by having a secondary continuum (matrix) coupled to the primary continuum (fracture) modeled as a disconnected one-dimensional domain using a method known as the Dual Continuum Disconnected Matrix (DCDM) model [27]. Advection and diffusion are allowed in the primary continuum, and in the secondary continuum transport occurs through diffusion only.

One limiting factor of the previous model was that only aqueous transport in the matrix was being accounted for. However, the multiple continuum model was recently updated to include gas phase matrix diffusion.

The equations for the primary and secondary continuum are solved in a coupled implementation. The primary continuum with gas transport is modeled via,

$$\frac{\partial}{\partial t}\epsilon_f\varphi_f(s^{aq}\Psi_j^{aq,f} + s^g\Psi_j^{g,f}) + \nabla\cdot(\Omega_j^{aq,f} + \Omega_j^{g,f}) = -A_{fm}(\Omega_j^{aq,fm} + \Omega_j^{g,fm}) - \epsilon_f\sum_k \nu_{jk}\Gamma_k^f$$

where superscript f and m denote the fracture and matrix continua, respectively, ϵ_f is the fracture volume fraction, φ^f is fracture porosity, s^{aq} and s^g are the saturation in the aqueous and gas phases respectively, $\Psi_j^{aq,f}$ is the total component concentration in the aqueous phase in the fracture of species j, $\Psi_j^{g,f}$ is the total component concentration in the gas phase in the fracture of species j, $\Omega_j^{aq,f}$, $\Omega_j^{g,f}$ is total solute flux in the fracture in the aqueous and gas phase respectively, Ω_j^{fm} is total solute flux between the fracture and matrix, A_{fm} is the fracture-matrix interfacial area, ν_{jk} is the stoichiometric coefficient, and Γ_k^f is the mineral reaction. The secondary continuum with gas transport is modeled as:

$$\frac{\partial}{\partial t}\varphi_m\left(s^{aq}\Psi_j^{aq,m} + s^g\Psi_j^{g,m}\right) + \nabla_\xi\cdot(\Omega_j^{aq,m} + \Omega_j^{g,m}) = -\sum_k \nu_{jk}\Gamma_k^m$$

where φ^m is matrix porosity and the gradient operator ∇_ξ refers to the effective one-dimensional secondary continuum geometry. The equations for the primary and secondary continuum are solved separately and coupled together by the mass exchange flux assuming symmetry along the axis dividing them [28]:

$$\Omega_j^{aq,fm}(x,t) = \Omega_j^{aq,m}\left(\xi_{fm},x\,\middle|\,r\right)$$

$$\Omega_j^{g,fm}(x,t) = \Omega_j^{g,m}\left(\xi_{fm},x\,\middle|\,r\right)$$

where x is a point in the primary continuum, t is time, and ξ_{fm} is the outer boundary of the secondary continuum. The model was additionally verified and validated against several analytical solutions and benchmarks which are documented in the PFLOTRAN Development Report FY2022 [29].

An example barometric pumping problem was created using the multiple continuum model. The problem consists of Xe transport originating approximately 105 m below the surface in a vertical fracture with a width of ~0.1 mm, where diffusion occurs into the rock matrix. A time-varying barometric pressure boundary condition was applied at the surface (Figure 4-1) and an initial pulse of approximately 4.4×10^{-12} bar of Xe was set at a depth of 75 m and then modeled for 900 days. The initial concentration of Xe was zero at all other locations including the secondary continuum (rock matrix). The primary continuum was set up with 110 cells where each cell had 100 cells in the secondary with a matrix length of 10.999 m. Table 1 lists the secondary continuum block added to the material properties block and values used to model the diffusion into the matrix.

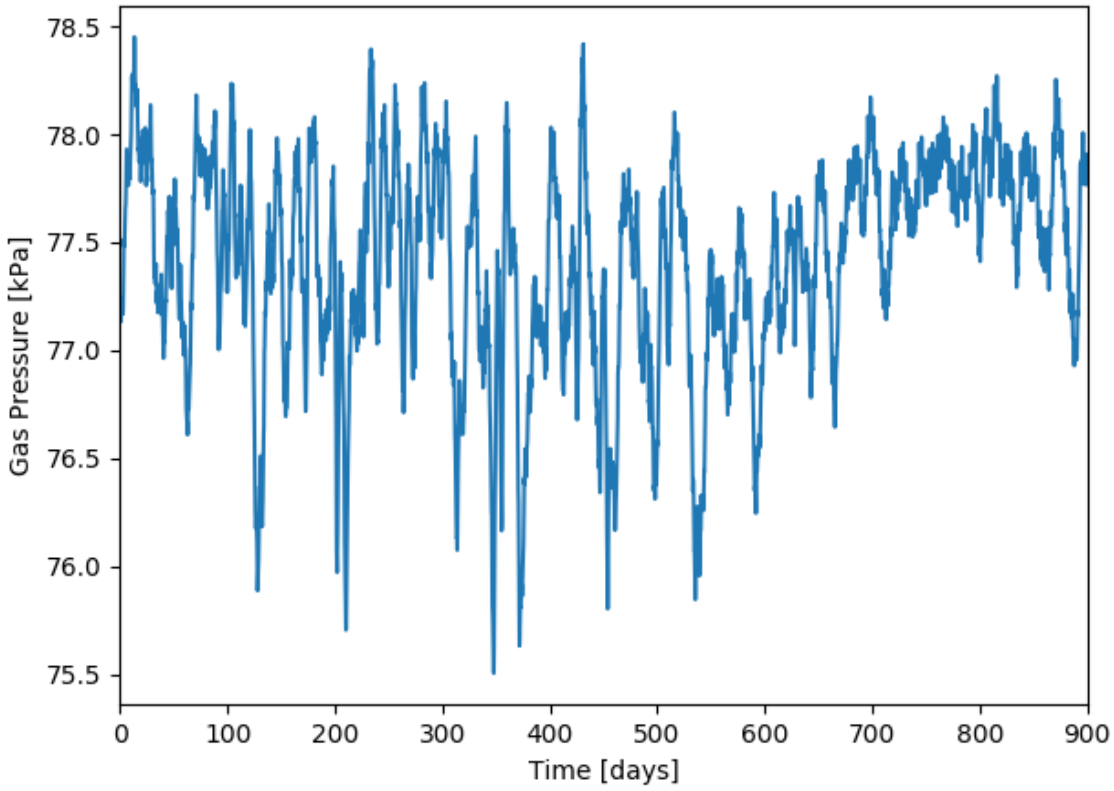

Figure 4-1. Time varying barometric pumping pressure boundary condition at surface.

Table 4-1. Example multi-continuum input deck values

Input	Value	Description
SECONDARY_CONTINUUM		Opens secondary continuum block in MATERIAL_PROPERTIES
TYPE	SLAB	Secondary continuum geometry
LENGTH	10.999	Half fracture spacing [m] (L) or desired length of matrix
NUM_CELLS	100	Number of cells in secondary continuum (per primary cell)
EPSILON	4.348E-6	Fracture volume fraction (can be specified as dataset for spatially varying epsilon). Calculated as: $b/(b+L)$, where b is half aperture and L is half fracture spacing.
LIQUID_DIFFUSION_COEFFICIENT	1.0E-9	Effective liquid diffusion coefficient [m^2/s] (includes tortuosity)
GAS_DIFFUSION_COEFFICIENT	1.0E-5	Effective gas diffusion coefficient [m^2/s] (includes tortuosity)
POROSITY	0.1	Porosity of the matrix

Partial pressure of Xe was plotted for several times along the fracture in Figure 4-2. Two different values of effective diffusion coefficients (gas and aqueous) were compared in the matrix. The solution was found to be very sensitive to the effective diffusion coefficient values, where a decrease in the effective diffusion coefficients showed a visible difference in partial pressures along the fracture at later times. Although gas retardation is not included in the multiple continuum model yet, future work includes adding in gas sorption capabilities and running large-scale tests on applied problems.

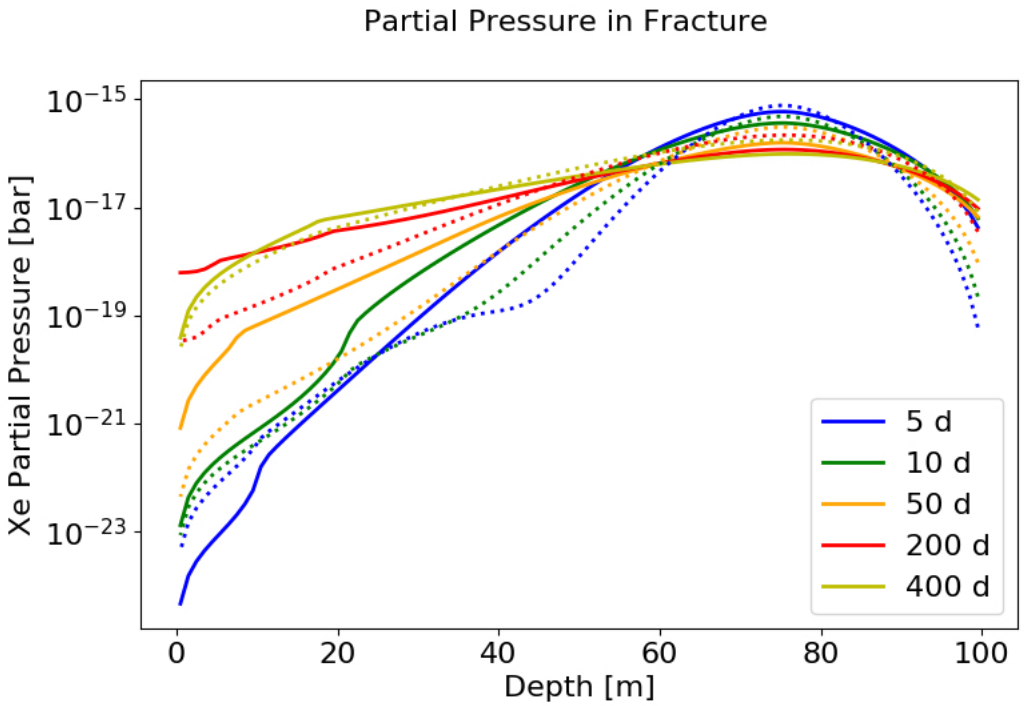

Figure 4-2. Xe partial pressure along the fracture for a matrix gas and liquid effective diffusion coefficient of 10^{-5} m^2/s and 10^{-9} m^2/s respectively (solid lines) and 3×10^{-5} m^2/s and 3×10^{-9} m^2/s (dashed lines) at various times during the simulation.

5. CONCLUSIONS

The retention factor approach developed here enables efficient modeling of the additional adsorbed phase of non-ideal tracer gases in porous media using the existing finite volume approach in PFLOTRAN. The approach is valid where the dilute transport approximation is valid, that is, where the tracer gas is present at low enough concentrations that it does not appreciably alter the bulk flow properties. While developed to model the transport of isotopic and chemical tracer gases, this approach may have broader application to dilute contaminants such as volatile organics (VOCs) and per- and polyfluoroalkyl substances (PFAS).

The adsorbed quantity is typically a complex multivariable function of gas composition in multicomponent systems. However, where the dilute transport approximation is valid, a linearization around the carrier gas composition is appropriate. This greatly simplifies the simulation relative to comprehensive but complex multicomponent models. At the same time, the gas adsorption transport model developed here is not suitable where the flow species are appreciably adsorbing, *e.g.,* hydrocarbons in shale gas reservoirs or carbon dioxide sequestration.

With a validated and verified model, more complex, heterogenous systems with tracer gas adsorption can now be modeled. This includes retardation and dispersion of adsorbing tracers in fractures surrounded by a porous matrix, which is relevant to the barometric pumping of contaminant gases from underground nuclear explosions.

This page left blank

REFERENCES

[1] P. Burnard, Ed., The Noble Gases as Geochemical Tracers, Berlin: Springer-Verlag Berlin Heidelberg, 2013.

[2] A. Turk, S. Edmonds, H. Mark and G. Collin, "Sulfur Hexafluoride as a Gas-Air Tracer," *Environ Sci Technol,* vol. 2, no. 1, pp. 44-48, 1968.

[3] E. D. Thimons and F. N. Kissel, "Tracer Gas as an Aid in Mine Ventilation Analysis," US Department of the Interior: Bureau of Mines, 1974.

[4] D. K. Kreamer, E. P. Weeks and G. M. Thompson, "A field technique to measure the tortuosity and sorption-affected porosity for gaseous diffusion of materials in the unsaturated zone with experimental results from near Barnwell, South Carolina," *Water Resourc Res,* vol. 24, no. 3, pp. 331-341, 1988.

[5] C. R. Carrigan, "The Non-Proliferation Experiment and Gas Sampling as an On-site Inspection Activity: A Progress Report," in *Symposium on the Non-Proliferation Experiment: Results and Implications for Test Ban Treaties*, Rockville, MD, 1994.

[6] C. R. Carrigan, R. A. Heinle, G. B. Hudson, J. J. Nitao and J. J. Zucca, "Trace gas emissions on geological faults as indicators of underground nuclear testing," *Nature,* vol. 382, pp. 528-531, 1996.

[7] K. Olsen *et al.*, "Noble gas migration experiment to support the detection of underground nuclear explosions," *J Radioanal Nucl Chem,* vol. 307, pp. 2603-2610, 2015.

[8] C. Johnson *et al.*, "Migration of noble gas tracers at the site of an underground nuclear explosion at the Nevada National Security Site," *J Environ Radioact,* Vols. 208-209, 2019.

[9] IUPAC, "IUPAC-NIST SOLUBILITY DATA SERIES," 18 February 2015. [Online]. Available: http://dx.doi.org/10.18434/T4QC79 .

[10] P. C. Lichtner *et al.*, "PFLOTRAN User Manual," 2020. [Online]. Available: http://documentation.pflotran.org.

[11] I. Langmuir, "The Adsorption of Gases on Plane Surfaces of Glass, Mica and Platinum," *J Am Chem Soc,* vol. 40, no. 9, pp. 1361-1403, 1918.

[12] N. Chakraborty, X. Lou, K. Enab and Z. Karpyn, "Measurement of In-situ Fluid Density in Shales with Sub-Resolution Porosity Using X-Ray Microtomography," *Transp Porous Media,* vol. 141, pp. 607-627, 2022.

[13] S. Brunauer, P. H. Emmett and E. Teller, "Adsorption of Gases in Multimolecular Layers," *J Am Chem Soc,* vol. 60, no. 2, pp. 309-319, 1938.

[14] F. P. Fanale and W. A. Cannon, "Physical Adsorption of Rare Gas on Terrigenous Sediments," *Earth and Planetary Science Letters,* vol. 11, pp. 362-368, 1871.

[15] G. W. Rattray, R. G. Striegl and I. C. Yang, "Adsorption of Sulfur Hexafluoride onto Crushed Tuffs from the Yucca Mountain Area, Nye County, Nevada," US Department of the Interior: US Geological Survey, Denver, CO, 1995.

[16] M. Paul and J. Feldman, " Measuring Gas Transport and Sorption in Large Intact Geologic Specimens via the Piezometric Method," *Transport in Porous Media,* vol. 139, pp. 1-20, 2021.

[17] J. Feldman, M. Paul, G. Xu, D. X. Rademacher, J. Wilson and T. M. Nenoff, "Effects of natural zeolites on field-scale geologic noble gas transport," *J Environ Radioact,* Vols. 220-221, 2020.

[18] C. W. Neil *et al.*, "Gas diffusion through variably-water-saturated zeolitic tuff: Implicaitons for transport following a subsurface nuclear event," *J Environ Radioact,* vol. 250, 2022.

[19] E. C. Jong, P. V. Macek, I. E. Perera, K. D. Luxbacher and H. M. McNair, "An Ultra-Trace Analysis Technique for SF6 Using Gas Chromatography with Negative Ion Chemical Ionization Mass Spectrometry," *J Chromatogr Sci,* vol. 53, no. 6, pp. 854-859, 2015.

[20] J. E. Heath, K. L. Kuhlman, S. T. Broome, J. E. Wilson and B. Malama, "Heterogeneous multiphase flow properties of volcanic rocks and implication for noble gas transport from underground nuclear explosions," *Vadose Zone J,* vol. 20, no. 3, 2021.

[21] D. C. Thorstenson and D. W. Pollock, "Gas transport in unsaturated porous media: The adequacy of Fick's law," *Rev Geophys,* vol. 27, no. 1, pp. 61-78, 1989.

[22] R. M. Barrer and L. V. C. Rees, "Henry's Law Adsorption Constants," *Trans Faraday Soc,* vol. 57, pp. 999-1007, 1961.

[23] A. Seiman, N. Makarõtševa, M. Vaher and M. Kaljurand, "The detection of nerve agent degradation products in different soil fractions using capillary electrophoresis with contactless conductivity detection," *Chem Ecol,* vol. 26, pp. 145-155, 2010.

[24] H. Freundlich, Kapillarchemie, Leipzig: Akademische verlagsgesellschaft, 1909.

[25] A. Myers and J. M. Prausnitz, "Thermodynamics of Mixed Gas Adsorption," *AIChE J,* vol. 11, pp. 121-130, 1965.

[26] R. Krishna and J. M. van Baten, "How Reliable Is the Ideal Adsorbed Solution Theory for the Estimation of Mixture Separation Selectivities in Microporous Crystalline Adsorbents?," *ACS Omega,* vol. 6, no. 23, pp. 15499-15513, 2021.

[27] P. Lichtner, "Critique of dual continuum formulations of multicomponent reactive transport in fractured porous media," in *Dyanmics of Fluids in Fractured Rock*, Washington, DC, American Geophysical Union, 2000, pp. 281-298.

[28] A. Iraola, P. Trinchero, S. Karra and J. Molinero, "Assessing dual continuum method for multicomponent reactive transport," *Comput Geosci,* vol. 130, pp. 11-19, 2019.

[29] M. Nole *et al.*, "PFLOTRAN Development FY2022," Sandia National Laboratories, 2022.

APPENDIX A. VERIFICATION PFLOTRAN INPUT DECK

```
SIMULATION
  SIMULATION_TYPE SUBSURFACE
  PROCESS_MODELS
    SUBSURFACE_FLOW flow
      MODE GENERAL
      OPTIONS
        RESTRICT_STATE_CHANGE
        IMMISCIBLE
      /
    END

    SUBSURFACE_TRANSPORT transport
      MODE GIRT
      OPTIONS
        SKIP_RESTART
      /
    END

  /
  RESTART gcbase-restart.h5 0.d0
END


SUBSURFACE

NUMERICAL_METHODS flow
  NEWTON_SOLVER
    USE_INFINITY_NORM_CONVERGENCE
    PRESSURE_CHANGE_LIMIT 5.d6
  /
END

NUMERICAL_METHODS transport
  NEWTON_SOLVER
    RTOL 1.d-10
    ATOL 1.d-12
    STOL 1D-30
    MAXIMUM_NUMBER_OF_ITERATIONS 100
    MAXF 1000
    MINIMUM_NEWTON_ITERATIONS 3
  /
  TIMESTEPPER TRANSPORT
    TS_ACCELERATION 32
  END

  LINEAR_SOLVER
    RTOL 1.d-12
    ATOL 1.d-12
    LU_ZERO_PIVOT_TOL 1.d-15
  /
END
```

```
EOS WATER
  DENSITY IF97
  ENTHALPY IF97
  STEAM_DENSITY IF97
  STEAM_ENTHALPY IF97
/
EOS GAS
  DENSITY IDEAL
/

#======================= chemistry

CHEMISTRY
  PRIMARY_SPECIES
    Xe(aq)
    SF6(aq)
    CF4(aq)
  END
  ACTIVE_GAS_SPECIES
    GAS_TRANSPORT_IS_UNVETTED
    Xe(g)
    SF6(g)
    CF4(g)
  END
  PASSIVE_GAS_SPECIES
    Xe(g)
    SF6(g)
    CF4(g)
  END
  AQUEOUS_DIFFUSION_COEFFICIENTS
   Xe(aq)  1.5e-5 cm^2/sec
   SF6(aq) 1.5e-5 cm^2/sec
   CF4(aq) 1.5e-5 cm^2/sec
  END

  GAS_DIFFUSION_COEFFICIENTS
    Xe(g)  0.124 cm^2/sec
    SF6(g) 0.124 cm^2/sec
    CF4(g) 0.124 cm^2/sec
  END
  SORPTION
    ISOTHERM_REACTIONS
      Xe(aq)
        DISTRIBUTION_COEFFICIENT 0.d0
      END
      SF6(aq)
        DISTRIBUTION_COEFFICIENT 0.d0
      END
      CF4(aq)
        DISTRIBUTION_COEFFICIENT 0.D0
      END
    END
  END
  GAS_SORPTION
    ISOTHERM_REACTIONS
      Xe(g)
        RETENTION_FACTOR 1.d0
```

```
      END
      SF6(g)
      RETENTION_FACTOR 0.d0
      END
      CF4(g)
        RETENTION_FACTOR 1.D1
      END
    END
  END


  DATABASE hanford_wSF6_wCF4.dat
  LOG_FORMULATION
  OUTPUT
    PRIMARY_SPECIES
    GASES
    TOTAL
    KD
    TOTAL_SORBED
  END

END

#========================== times
TIME
  FINAL_TIME 4.d6 s
  INITIAL_TIMESTEP_SIZE 1.d-9 s
  MAXIMUM_TIMESTEP_SIZE 5.d3 s
END

FLUID_PROPERTY
  PHASE LIQUID
  DIFFUSION_COEFFICIENT 0.d0
END

FLUID_PROPERTY
  PHASE GAS
  DIFFUSION_COEFFICIENT 0.d0
END

#========================== discretization
GRID
  TYPE STRUCTURED
  NXYZ 220 1 1
  BOUNDS
    0.d0 0.d0 0.d0
    110.d0 1.d1 1.d1
  END
END

#========================== output options
OUTPUT

  VARIABLES
    GAS_SATURATION
    GAS_PRESSURE
    GAS_DENSITY
```

```
    GAS_MOBILITY
    POROSITY
    PERMEABILITY
    GAS_MOLE_FRACTIONS
    VAPOR_PRESSURE
    LIQUID_MOLE_FRACTIONS
    LIQUID_PRESSURE
    LIQUID_SATURATION
    TEMPERATURE
    THERMODYNAMIC_STATE
    MATERIAL_ID
    CAPILLARY_PRESSURE
  END
  SNAPSHOT_FILE
    PERIODIC TIME 50000 s between 0.0 s and 4.d6 s
    FORMAT HDF5
    VELOCITY_AT_CENTER
  END
  SNAPSHOT_FILE
    PERIODIC TIME 50000 s between 0.0 s and 4.d6 s
    FORMAT TECPLOT POINT
  END
  MASS_BALANCE_FILE
    PERIODIC TIME 50000 s between 0.0 s and 4.d6 s
    TOTAL_MASS_REGIONS
      all
    /
  END
END

#========================== materials/characteristic curves

MATERIAL_PROPERTY sandstone
  ID 1
  CHARACTERISTIC_CURVES default
  POROSITY 0.20
  !TORTUOSITY 0.20
  TORTUOSITY_FUNCTION_OF_POROSITY 0.333 #Millington and Quirk
  SOIL_COMPRESSIBILITY 3.2d-9 #1/Pa, what Payton used in 2015 clay case
  SOIL_COMPRESSIBILITY_FUNCTION LEIJNSE
  SOIL_REFERENCE_PRESSURE 101325.d0
  ROCK_DENSITY 2700.
  THERMAL_CONDUCTIVITY_DRY 1.0d0 #complete guess
  THERMAL_CONDUCTIVITY_WET 3.1d0 #Forster and Merriam 197, Dakota sandstone
  HEAT_CAPACITY 830.
  PERMEABILITY
    PERM_ISO 20.d-12
  /
/

CHARACTERISTIC_CURVES default
  SATURATION_FUNCTION VAN_GENUCHTEN
    ALPHA 1.d-4
    M 0.5
    LIQUID_RESIDUAL_SATURATION 0.1d0
    MAX_CAPILLARY_PRESSURE 1.d7
  /
```

```
  PERMEABILITY_FUNCTION MUALEM_VG_LIQ
    PHASE LIQUID
    M 0.5
    LIQUID_RESIDUAL_SATURATION 0.1d0
  /
  PERMEABILITY_FUNCTION MUALEM_VG_GAS
    PHASE GAS
    M 0.5
    LIQUID_RESIDUAL_SATURATION 0.1d0
    GAS_RESIDUAL_SATURATION 0.1d0
  /
END

#========================== regions
REGION all
  COORDINATES
   -1.0D+20 -1.0D+20 -1.0D+20
    1.0D+20  1.0D+20  1.0D+20
  /
END

REGION west
  FACE WEST
  COORDINATES
    0.d0 0.d0 0.d0
    0.d0 1.d1 1.d1
  /
END

REGION inj
  COORDINATES
    5.D0 5.D0 5.D0
  /
END

REGION east
  FACE EAST
  COORDINATES
    110.d0 0.d0 0.d0
    110.d0 1.d1 1.d1
  /
END
# ====================== flow condition
FLOW_CONDITION initial
  TYPE
    TEMPERATURE DIRICHLET
    GAS_PRESSURE DIRICHLET
    GAS_SATURATION DIRICHLET
  END
  TEMPERATURE 2.5d1
  GAS_PRESSURE 1.d5
  GAS_SATURATION 9.99999d-1
END

FLOW_CONDITION west
  TYPE
    TEMPERATURE DIRICHLET
```

```
    GAS_PRESSURE DIRICHLET
    GAS_SATURATION DIRICHLET
  END
  TEMPERATURE 2.5d1
  GAS_PRESSURE 1.1d5
  GAS_SATURATION 9.99999d-1
END

CONSTRAINT initial
  CONCENTRATIONS
    Xe(aq)  1.00D-40 G   Xe(g)
    SF6(aq) 1.00D-40 G SF6(g)
    CF4(aq) 1.00D-40 G CF4(g)
  END
END

TRANSPORT_CONDITION initial
  TYPE DIRICHLET_ZERO_GRADIENT
  CONSTRAINT_LIST
    0.0D+0 initial
  END
/

FLOW_CONDITION outlet
  TYPE
    RATE mass_rate
  /
  RATE 0.d0 -8.0215d-7 0.d0 kg/s kg/s W
/
CONSTRAINT inj
  CONCENTRATIONS
    Xe(aq)  4.42e-12 G  Xe(g)
    SF6(aq) 8.84e-12 G SF6(g)
    CF4(aq) 0.8036e-12 G CF4(g)
  END
END

TRANSPORT_CONDITION inj
  TYPE DIRICHLET_ZERO_GRADIENT
  CONSTRAINT_LIST
    0.0D+0 inj
  END
END

INITIAL_CONDITION initial
  FLOW_CONDITION initial
  TRANSPORT_CONDITION initial
  REGION all
END

INITIAL_CONDITION pulse
  FLOW_CONDITION initial
  TRANSPORT_CONDITION inj
  REGION inj
END

BOUNDARY_CONDITION west
```

```
  FLOW_CONDITION west
  TRANSPORT_CONDITION initial
  REGION west
END

BOUNDARY_CONDITION east
  FLOW_CONDITION initial
  TRANSPORT_CONDITION initial
  REGION east
END

STRATA
  REGION all
  MATERIAL sandstone
END

END_SUBSURFACE
```

This page left blank

DISTRIBUTION

Email—Internal

Name	Org.	Sandia Email Address
Stephanie Eras	6756	sjeras@sandia.gov
Stephanie Teich-McGoldrick	6756	steichm@sandia.gov
Jeffery Greathouse	8842	jagreat@sandia.gov
Kristopher Kuhlman	8842	klkuhlm@sandia.gov
Matthew Paul	8842	matpaul@sandia.gov
David Fukuyama	8844	defukuy@sandia.gov
Rosemary Leone	8844	rleone@sandia.gov
Michael Nole	8844	mnole@sandia.gov
Kyle Jones	8911	krjones@sandia.gov
Scott Broome	8914	stbroom@sandia.gov
Technical Library	1911	sanddocs@sandia.gov

Email—External

Name	Company Email Address	Company Name
Glenn Hammond	glenn.hammond@pnnl.gov	Pacific Northwest National Laboratory
Peter Lichtner	plichtner@unm.edu	University of New Mexico

Sandia National Laboratories

Sandia National Laboratories is a multimission laboratory managed and operated by National Technology & Engineering Solutions of Sandia LLC, a wholly owned subsidiary of Honeywell International Inc. for the U.S. Department of Energy's National Nuclear Security Administration under contract DE-NA0003525.